View metadata, citation and similar papers at core.ac.uk
brought to you by CORE
provided by Elsevier - Publisher Connector

Cell PRESS
Structure
Article

Dynamic and Structural Characterization of a Bacterial FHA Protein Reveals a New Autoinhibition Mechanism

Philippe Barthe,[1,2,3] Christian Roumestand,[1,2,3] Marc J. Canova,[4] Laurent Kremer,[5,6] Corinne Hurard,[1,2,3] Virginie Molle,[4] and Martin Cohen-Gonsaud[1,2,3,*]
[1]Centre National de la Recherche Scientifique Unité Mixte de Recherche (CNRS UMR) 5048, Centre de Biochimie Structurale, Montpellier, France
[2]Institut National de la Santé et de la Recherche Médicale U554, Montpellier, France
[3]Université Montpellier I et II, Montpellier, France
[4]Institut de Biologie et Chimie des Protéines, CNRS UMR 5086, Université Lyon 1, IFR128 BioSciences, Lyon-Gerland, Lyon, France
[5]Laboratoire de Dynamique des Interactions Membranaires Normales et Pathologiques, Universités de Montpellier II et I, CNRS UMR 5235, Case 107, Place Eugène Bataillon, 34095 Montpellier Cedex 05, France
[6]Institut National de la Santé et de la Recherche Médicale, Dynamique des Interactions Membranaires Normales et Pathologiques, Place Eugène Bataillon, 34095 Montpellier Cedex 05, France
*Correspondence: martin@cbs.cnrs.fr
DOI 10.1016/j.str.2009.02.012

SUMMARY

The OdhI protein is key regulator of the TCA cycle in *Corynebacterium glutamicum*. This highly conserved protein is found in GC rich Gram-positive bacteria (e.g., the pathogenic *Mycobacterium tuberculosis*). The unphosphorylated form of OdhI inhibits the OdhA protein, a key enzyme of the TCA cycle, whereas the phosphorylated form is inactive. OdhI is predicted to be mainly a single FHA domain, a module that mediates protein-protein interaction through binding of phosphothreonine peptides, with a disordered N-terminal extension substrate of the serine/threonine protein kinases. In this study, we solved the solution structure of the unphosphorylated and phosphorylated isoforms of the protein. We observed a major conformational change between the two forms characterized by the binding of the phosphorylated N-terminal part of the protein to its own FHA domain, consequently inhibiting it. This structural observation corresponds to a new autoinhibition mechanism described for a FHA domain protein.

INTRODUCTION

Reversible protein phosphorylation is a key mechanism by which environmental signals are transmitted to modify protein expression or activity in eukaryotes and prokaryotes, and therefore represents a crucial mechanism by which exogenous signals are translated into cellular responses. Eukaryotic-like Ser/Thr protein kinases (STPKs) present in bacteria are thought to play important functions in cell signaling responses as well as in essential metabolic pathways. However, understanding prokaryotic kinase biology has been hampered by the failure to identify relevant kinase substrates and subsequently characterize the phosphorylation site(s). In addition, very little is known about how phosphorylation induces structural modifications in STPK substrates, ultimately leading to changes in the biological responses in bacteria.

Corynebacterium glutamicum is a nonpathogenic Gram-positive bacterium used for industrial production of L-glutamate and other amino acids (Kimura, 2003) and represents a valuable model organism to study Corynebacteriaceae, a suborder of actinomycetes that includes *Mycobacterium* (Alderwick et al., 2005). Recent studies have brought to light an unusual post-translational regulation mechanism of the tricarboxylic (TCA) cycle in *C. glutamicum* (Bott, 2007). In this organism, the 450 kDa 2-oxoglutarate dehydrogenase multienzyme complex (ODHC) catalyzes the fourth step of the TCA cycle, and regulation of ODHC activity was shown to be dependent on the OdhI (for ODHC inhibitor) phosphorylation status. In fact, the unphosphorylated form of OdhI binds with high-affinity to OdhA, the putative E1 subunit of the ODHC complex, thus inhibiting its activity, whereas OdhI phosphorylation relieves this inhibition (Niebisch et al., 2006). Regulation of the TCA cycle by phosphorylation of the isocitrate deshydrogenase has been reported in enteric bacteria (Cozzone, 1998). The channeling of isocitrate through the glyoxylate bypass is regulated via direct phosphorylation/dephosphorylation of the isocitrate dehydrogenase, the enzyme of the TCA cycle. However, in the present study, we characterize for the first time a novel way of controlling the TCA cycle via the 2-oxoglutarate dehydrogenase, which is not directly phosphorylated but regulated via a phosphorylation/dephosphorylation mechanism of its specific binding regulator, OdhI.

C. glutamicum contains four STPKs named *Cg*PknA, *Cg*PknB, *Cg*PknG, and *Cg*PknL (Kalinowski et al., 2003). Inactivation of *CgpknL* or *CgpknG* in *C. glutamicum* resulted in viable mutants with a normal cell morphology or growth rate. In sharp contrast, *CgpknA* and *CgpknB* were found to be essential (Fiuza et al., 2008). Partial deletion of *CgPknA* or *CgPknB* in conditional mutants resulted in elongated cells, leading to the conclusion

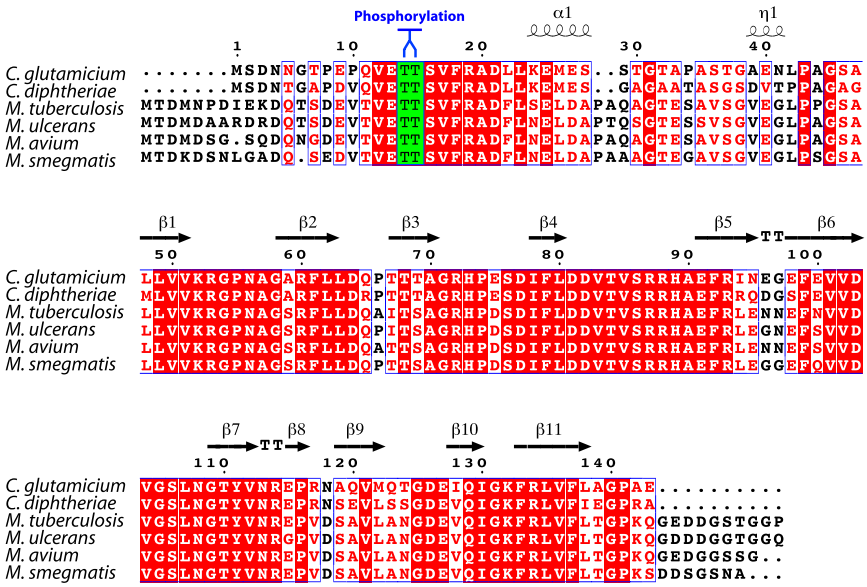

Figure 1. Multiple Sequence Alignment of OdhI Ortholog Proteins from Corynebacteria and Mycobacteria

Sequence alignment of the *Corynebacterium glutamicum* OdhI homologs in *Corynebacterium diphtheriae*, *Mycobacterium tuberculosis*, *Mycobacterium ulcerans*, *Mycobacterium avium*, and *Mycobacterium smegmatis*. The conserved Thr residues described in *M. tuberculosis* and *C. glutamicum* as the phosphorylation sites are highlighted in green. Protein secondary element assignments for the phosphorylated form of OdhI are represented on the top of the sequences. Numbering of amino acids corresponds to the OdhI protein from *C. glutamicum*.

that these two kinases are key players in signal transduction pathways controlling corynebacterial cell shape and growth. In addition, both *Cg*PknA and *Cg*PknB were able to phosphorylate OdhI in vitro (Fiuza et al., 2008), while OdhI was originally reported to be a substrate of *Cg*PknG (Niebisch et al., 2006).

OdhI is a 15 kDa protein, and structure prediction proposed that it is almost solely composed of a forkhead-associated (FHA) domain adjacent to an unfolded 40-residues N-terminal extension where phosphorylation occurs (Niebisch et al., 2006). FHA domains are modular recognition domains highly specific to phosphothreonine and participating in various biological processes such as transcription, DNA repair, or protein degradation in eukaryotes (Durocher and Jackson, 2002). This FHA-containing protein is highly conserved in actinomycetes, suggesting that it plays an important role in the physiology of these organisms. In *M. tuberculosis*, the OdhI ortholog named GarA (Rv1827) shares 60% of sequence identity (82% for the FHA domain) with OdhI and has been partially characterized (Villarino et al., 2005). Like OdhI, GarA was found to be phosphorylated by mycobacterial STPKs on an N-terminal threonine residue (Villarino et al., 2005). Conservation of OdhI with GarA, and OdhA with its *M. tuberculosis* ortholog KGD (Rv1248c), leads to the hypothesis of common functions and regulatory mechanisms. Recent studies have unraveled a role for GarA in regulation of glutamate metabolism and demonstrated that both *M. tuberculosis* PknB and PknG were able to phosphorylate GarA (O'Hare et al., 2008). Interestingly, *M. tuberculosis* PknG phosphorylates GarA at Thr21, adjacent to the residue phosphorylated by PknB (T22), and that these two phosphorylation events are mutually exclusive, supporting the occurrence of a site-specific kinase-dependent mechanism.

Because in OdhI only Thr14 (the equivalent of Thr21 in GarA) has been uncovered following phosphorylation with *Cg*PknG, we addressed whether the adjacent residue Thr15 (the equivalent of Thr22 in GarA) could also represent a potential phosphorylation site for *Cg*PknA or *Cg*PknB. We therefore identified the phosphorylated site(s) of OdhI by mass spectrometry analysis following phosphorylation with either *Cg*PknA or *Cg*PknB. Then, to decipher the molecular mechanism responsible for the release of the inhibition on OdhA via OdhI, as well as the binding properties of the OdhI regulator after phosphorylation, we determined the solution structures of both unphosphorylated (OdhI) and phosphorylated isoforms of OdhI (pOdhI) using multidimensional nuclear magnetic resonance (NMR) techniques. Our study unraveled a new structural mechanism in which the unstructured N-terminal segment of OdhI undergoes considerable conformational changes upon phosphorylation by *Cg*PknA or *Cg*PknB. These changes comprise a switch of the N-terminal part of the protein in close vicinity to the FHA domain phosphopeptide binding site. Herein, we describe an original mechanism of autoinhibition of OdhI and provide a structural model describing how phosphorylation of a single Thr residue in a disordered domain affects the overall structure of a protein, ultimately conditioning the regulation of a major metabolic pathway.

RESULTS

C. glutamicum PknA/B Phosphorylate OdhI on Thr15

The OdhI/GarA family of proteins appears to be conserved in actinomycetes, and close members of this family have been found in *Corynebacterium*, *Mycobacterium*, *Rhodococcus*, and *Streptomyces*. Figure 1 presents multiple sequence alignments of OdhI proteins in several corynebacterial and mycobacterial species, including pathogenic and nonpathogenic species. *C. glutamicum* contains four STPKs named *Cg*PknA, *Cg*PknB, *Cg*PknG, and *Cg*PknL (Kalinowski et al., 2003). It was previously demonstrated that a *C. glutamicum* strain lacking a functional *Cg*PknG was impaired in glutamine utilization. Subsequent proteome analysis led to the identification of OdhI, a 15 kDa protein, as a substrate of *Cg*PknG (Niebisch et al., 2006). Moreover, *Cg*PknG was shown to phosphorylate OdhI at position Thr14. A recent study dedicated to characterize the four corynebacterial STPKs reported that both *Cg*PknA and *Cg*PknB could efficiently phosphorylate OdhI in vitro in addition to *Cg*PknG (Fiuza et al., 2008). This protein was found to be highly homologous to the *M. tuberculosis* GarA protein (Villarino et al., 2005). Interestingly, O'Hara et al. (2008) demonstrated that *M. tuberculosis*

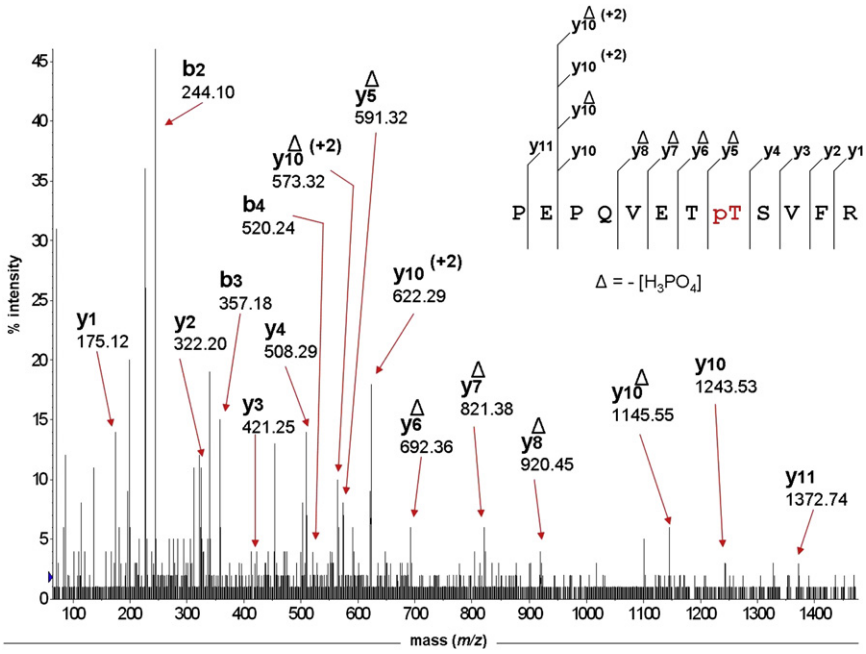

Figure 2. MS/MS Spectrum of the Triply Charged Ion $[M+3H]^{3+}$ at m/z 1059.8 of Peptide [8–19] (Monoisotopic Mass: 3176.38 Da)

Unambiguous location of the phosphate group on Thr15 was showed by observation of the "y" C-terminal daughter ion series. Starting from the C-terminal residue, all "y" ions loose phosphoric acid (−98 Da) after the Thr15 phosphorylated residue.

PknG phosphorylates GarA at Thr21, adjacent to the residue phosphorylated by PknB (Thr22), and that these two phosphorylation events are mutually exclusive. These unexpected findings brought us to investigate whether *Cg*PknA and *Cg*PknB phosphorylate OdhI on Thr14, like *Cg*PknG, or on Thr15. To this aim, a mass spectrometry technique was successfully developed to decipher the phosphorylation site(s). Purified recombinant OdhI was incubated with ATP in the presence of *Cg*PknA, and subjected to mass spectrometry analysis after tryptic digestion. ProteinPilot® database-searching software (version 2.0, Applied Biosystems), using the Paragon method with phosphorylation emphasis, was used to detect and identify the phosphorylated peptides. The sequence coverage of the protein was 99%, and MS/MS spectrum of the triply charged ion $[M+3H]^{3+}$ at m/z 1059.8 of peptide [8–19] (monoisotopic mass: 3176.38 Da) unambiguously confirmed the location of the phosphate group on Thr15 as showed by observation of the "y" C-terminal daughter ion series (Figure 2). Moreover, similar MS spectra were obtained when OdhI was phosphorylated with *Cg*PknB alone, or with a mix *Cg*PknA/*Cg*PknB (data not shown). Overall, these results indicate that *Cg*PknA or *Cg*PknB phosphorylate OdhI on Thr15, which is adjacent to the residue phosphorylated by *Cg*PknG (Thr14). This scenario is reminiscent of what was reported for GarA in *M. tuberculosis* (O'Hare et al., 2008) and supports the occurrence of a site-specific kinase-dependent mechanism. Moreover, these results appear to suggest that corynebacterial and mycobacterial kinases share similar phosphorylation specificity toward their substrates OdhI or GarA, and could therefore be regarded as genuine functional orthologs.

NMR Structure of the Unphosphorylated Form of OdhI

$[^1H,^{15}N]$ heteronuclear single-quantum coherence (HSQC) spectrum of OdhI is shown in Figure 3. By combining the information from the double- and triple-resonance heteronuclear experiments, we were able to assign all the amide group resonances for the nonproline residues (9 prolines), 99.8% of the other backbone resonances (Cα, C′, and Hα), more than 93.8% of the Cβ resonances, and 91% of the side chain protons.

In agreement with our sequence analysis, NMR experiments revealed that the N-terminal part of the unphosphorylated OdhI protein is fully disordered (Met1-Glu40). The corresponding residues give rise to the intense cross-peaks centered at 8.5 ppm in the HSQC spectrum. The rest of the molecule folds in a well-defined FHA domain. The global fold of the FHA domain, a β sandwich composed of 11 strands, is well conserved (Figure 4A) and similar to what has been described for the structures of the human Chk2 kinase or Ki67 FHA domains (rmsd of 1.62 Å and 1.68 Å, respectively; Li et al., 2002, 2004). However, superimposition with other FHA domain structures in the free form or in complex with a phosphopeptide revealed a particular conformation of the phosphopeptide-binding surface composed of loops connecting the β strands, mainly the loops β3/β4, β4/β5, and β6/β7. In the previously solved FHA domain containing protein structures, the phosphopeptide-binding loops adopted the same conformation in both free and complexed forms (i.e., PDB1R21 versus PDB2AFF; see Figure S1A available online). Here, loop β6/β7 in the free form is at the position that would be normally occupied by the pThr in the complexed form (Figure S1B). Concomitantly, the β3/β4 loop adopts a conformation incompatible with the phosphopeptide binding, whereas the position of loop β6/β7 is similar to that observed in related FHA domain structures.

NMR Structure of the Phosphorylated Form of OdhI (pOdhI)

High phosphorylation yields were obtained by incubating purified ^{15}N-labeled OdhI with both purified *C. glutamicum* STPKs, *Cg*PknA and *Cg*PknB, prior to the NMR structure determination. An increased spectral dispersion due to important chemical shift variations was observed on the $[^1H,^{15}N]$ HSQC spectrum recorded after treatment with the kinases (Figures 5A and 5B). As a first important result, frequency resonance sequential attribution revealed a unique phosphorylation site on Thr15, easily identified by the characteristic downfield chemical shift change (Byeon et al., 2005) from Thr to pThr (2 ppm), and consistent with our MS analysis (Figure 2). In addition, an important number

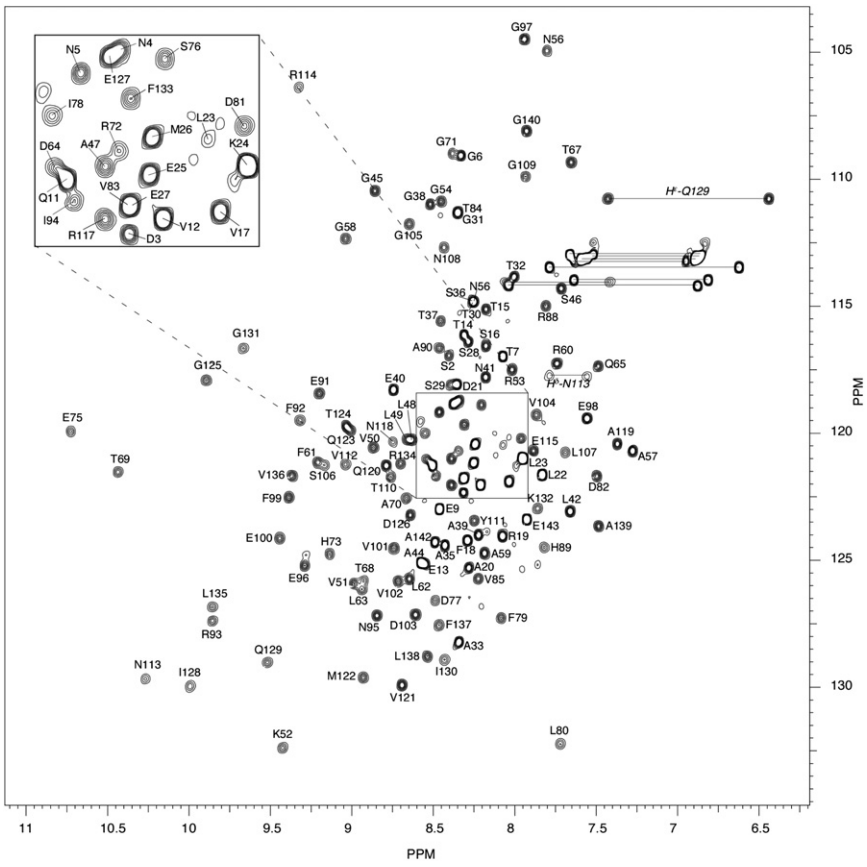

Figure 3. OdhI NMR Fingerprint

[^{1}H-^{15}N] HSQC spectrum of OdhI from *Corynebacterium glutamicum* recorded at 20°C on a ^{15}N uniformly labeled sample. Cross-peak assignments are indicated using the one-letter amino acid and number. The central part of the spectrum is expanded in the insert.

of intense peaks centered around 8.5 ppm in the ^{1}H dimension of the HSQC recorded on OdhI and attributed to mobile unfolded residues disappeared in the HSQC spectrum recorded on pOdhI. This suggests the structuring of a large part of the N-terminal residues upon phosphorylation. This was further confirmed by ^{15}N heteronuclear NMR relaxation experiments recorded on both isoforms of the protein. Although negative [^{1}H,^{15}N] heteronuclear NOE values were observed in the N-terminal segment (residues Met1 to Ala33) in the unphosphorylated form; positive values were observed around the putative phosphorylation site (residue Gln11 to Glu27) in the phosphorylated form of the protein (Figure 6). However, few chemical shift variations were observed for residues belonging to the FHA domain itself (Figures 5A and 5B), indicating that its structure is globally preserved, even though some perturbations are observed on the phosphothreonine binding site.

Structure calculation of the phosphorylated isoform of OdhI, pOdhI, confirms that phosphorylation induces folding of the N-terminal disordered region from residue Pro10 to Gly31 and triggers the binding of the region surrounding pThr15 to the FHA domain (Figures 4B–4D). More precisely, residues from Ala20 to Ser29 fold into a short α-helix, and residues from Val12 to Phe18 bind to the FHA phosphopeptide surface between loop β4/β5 and β3/β4. This positioning is consistent with the chemical shift perturbations observed on the pOdhI HSQC spectrum and with what has been observed in the previous structures of FHA domains in complex with phosphopeptides. The phosphorylation-induced α-helix is markedly amphipathic with a hydrophobic surface (Ala20, Leu22, Leu23, and Met26) facing Tyr111 and Pro116 on the β7 and the β8 FHA strands, respectively. These hydrophobic contacts, conserved in GarA, probably contribute to reinforce the interaction between the phosphorylated N-terminal peptides segment and the FHA binding site.

It has been reported that the minimum motif for recognition specificity is seven residues centered on the phosphothreonine (Durocher et al., 2000). Here, the phosphorylation results in the folding of 26 amino acids from the N-terminal, but only seven of them, centered on pThr15, are in contact with the FHA core domain according to our NMR data. The binding surface and the contacts between the phosphopeptide and its binding groove are original with an unusual dual interaction between the phosphate group and an arginine residue of loop β4/β5, Arg87. Recently a similar interaction has been described for the RNF8 FHA domain (Huen et al., 2007). The characteristic interaction described between the FHA domain and the phosphopeptide are conserved. The phosphate group is making hydrogen bounds with the buried Ser86 and additional hydrogen-bond interactions with main-chain atoms of residues from the phosphopeptide on both sides of the phosphothreonine are present. If not directly observable in our NMR experiments, some interaction is likely to be present. For instance, Arg72 guanidinium group from the Gly-Arg dipeptide motif, located at the N-terminal side of the β3/β4 loop, is expected to be doubly H-bonded to the phosphate group. In addition, the amide side chain of the highly conserved asparagine Asn107 should make hydrogen bonds with the main-chain carbonyl oxygen of the pThr +1 residue and the peptide nitrogen of pThr +3.

Similarly, α-helix formation upon phosphorylation has been previously reported for the hNIFK phosphopeptide after binding to the Ki67 FHA domain (Byeon et al., 2005). Multiple phosphorylations on this peptide and FHA domain binding are concomitant with the formation of a 15 aa α-helix beginning four residues after the first phosphorylated threonine. In our case, the α-helix tops the β strands β7 and β8, whereas the hNIFK peptide α-helix lies between loops β4/β5 and β10/β11 with the C-terminal part of the peptide forming an extra β strand antiparallel to β4.

The pOdhI structure clearly demonstrates an important molecular switch governed by a single phosphorylation event in a disordered domain.

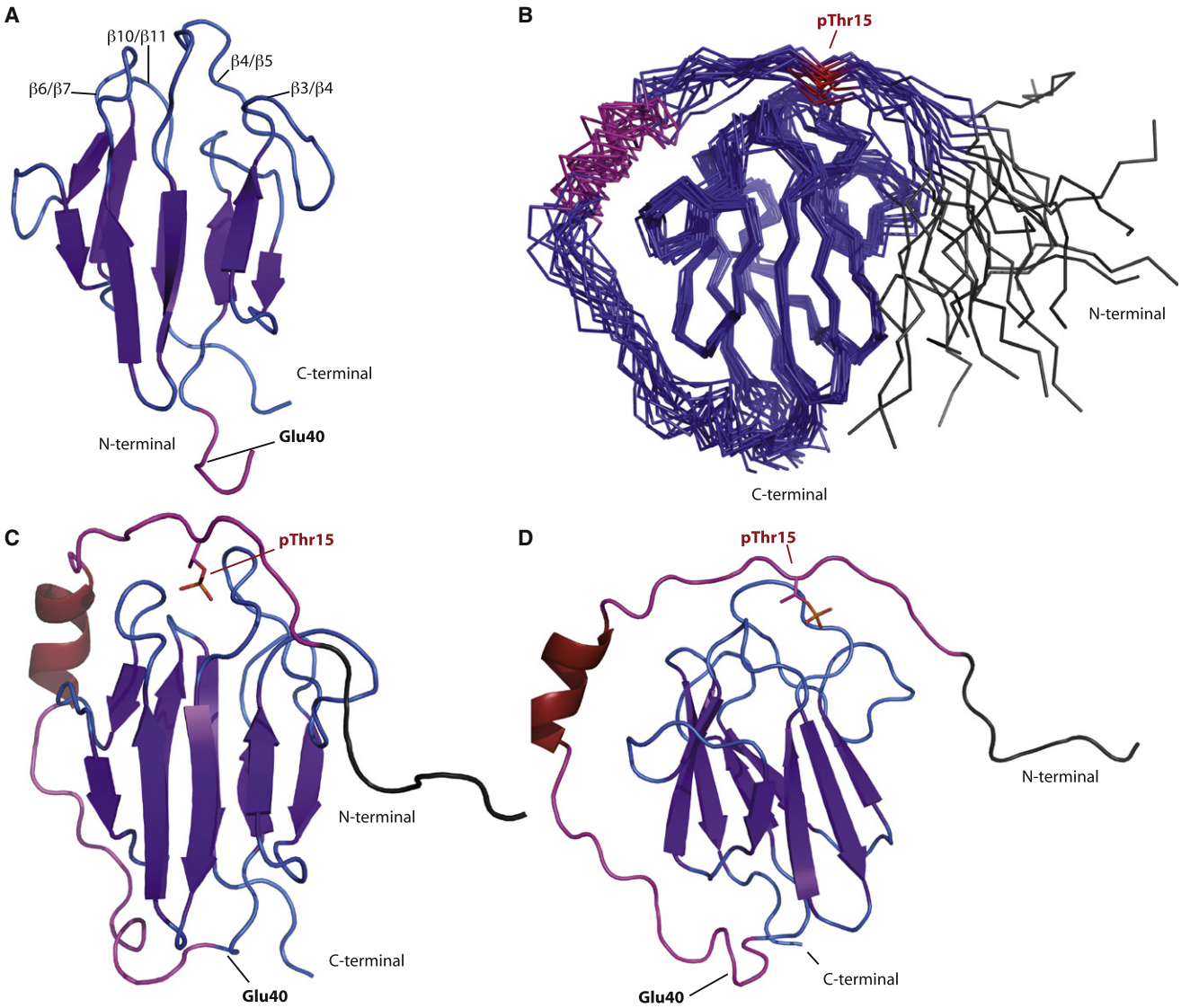

Figure 4. Overall Structure of the OdhI Structures

(A) Cartoon representation of the OdhI unphosphorylated structure. The N-terminal part of the protein from Met1 to Ala39 is fully disordered and not represented.

(B) Representation of the final ensemble comprising 30 NMR structures of the phosphorylated OdhI, pOdhI. The superimposition has been made on the core domain backbone atoms. The residues Met1 to Glu9 are not represented as they remain fully disordered in both structures. The residues from Pro10 to Ala39, unfolded in the unphosphorylated form, are represented wrapped around the FHA domain. The phosphothreonine anchoring in the FHA domain is represented in red, and the rest of the protein is in blue.

(C and D) Two views related by a 90° rotation along the z axis of a cartoon representation of the pOdhI structure. The residues Met1 to Glu9 are represented in gray, Pro10 to Ala39 are in red; side chain atoms of the phosphothreonine anchoring in the FHA domain are also represented.

DISCUSSION

In this study, the solution structure determination of OdhI isoforms revealed a major structural rearrangement in the phosphorylated isoform, characterized by a tight self-recognition binding of the phosphorylated N-terminal extension of the OdhI protein by the C-terminal FHA domain. Because phosphorylation of OdhI leads to a fully inactive protein unable to bind to OdhA, this intramolecular change accounts for an autoinhibition mechanism that shuts down the inhibition properties of OdhI (Figure 7). Morevover, an autoinhibition mechanism similar to the one described in this study has been recently reported for the *M. tuberculosis* OdhI homolog GarA, using a physicochemical strategy (England et al., 2009).

However, it remains unclear whether it is the phosphorylation and the binding of the N-terminal region that locks the FHA domain of OdhI, or if the inhibition results from the N-terminal part of OdhI becoming masked. The N-terminal sequence identity between the different species harboring OdhI/GarA orthologues is relatively low compared with the FHA domain itself (Figure 1). In addition, extensive sequence alignments of all the members of the family revealed that more-distant OdhI/GarA orthologs (sequence identity >60% for the FHA domain) lack

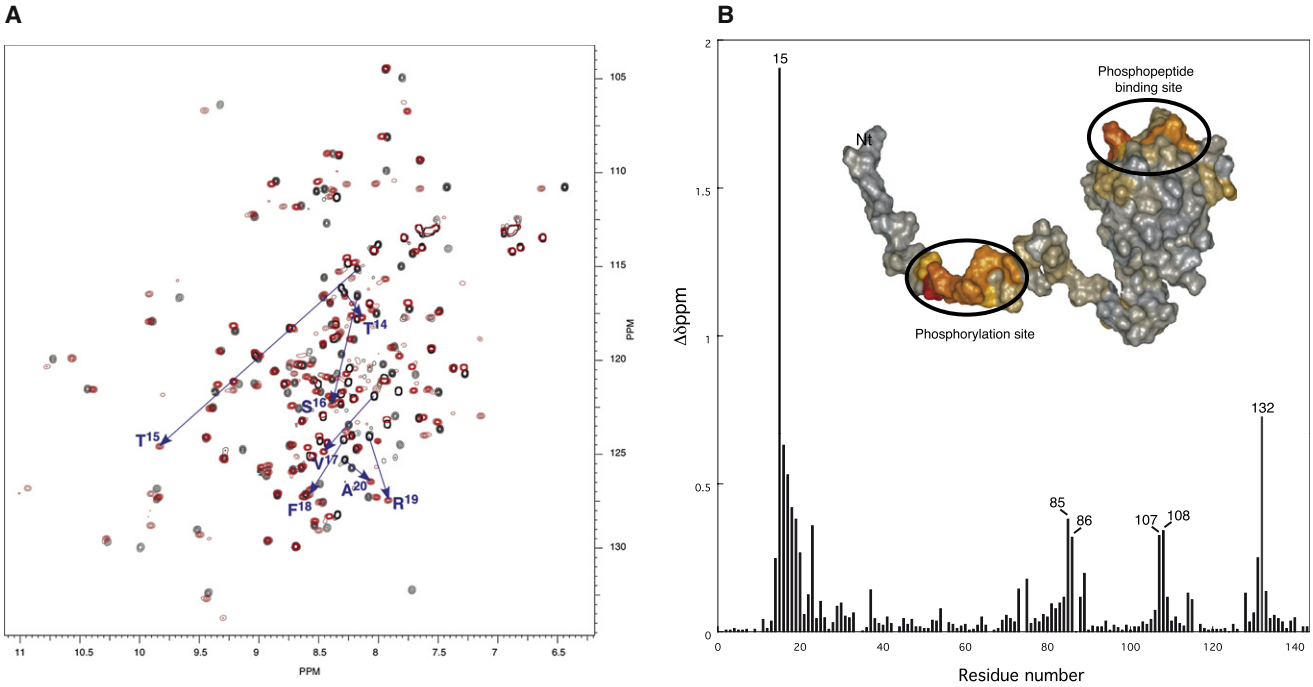

Figure 5. Chemical Shift Perturbations following OdhI Phosphorylation

(A) [^{1}H-^{15}N] HSQC spectrum superimposition of OdhI nonphosphorylated (in black) with pOdhI phosphorylated by *Cg*PknA/B (in red). Arrows connect resonances for the residues 14–20 in their position prior to and after phosphorylation.

(B) Amide averaged chemical shift differences (Δδ) as a function of the protein sequence. Δδ have been calculated between the amide group resonances of OdhI and pOdhI using $\Delta\delta = [\Delta\delta_H{}^2+(\Delta\delta_N.\gamma_N/\gamma_H)^2]^{0,5}$. The inserted panel presents the Van der Waals diagram of the OdhI NMR structure, with a color gradient indicative of the Δδ value: from gray ($\Delta\delta \approx 0$) to red ($\Delta\delta_{max}$ for Thr15). Ellipses indicate the phosphothreonine site and the phosphopeptide binding site.

the N-terminal part of the protein (data not shown). One possible explanation could be that in these species the FHA domain remains capable of inhibiting the TCA cycle, but may no longer be controlled by STPK-dependent phosphorylation. Moreover, considering the high value of the inhibitory constant (K_i = 2.4 nM and IC_{50} = 4.3 nM; Niebisch et al., 2006), we propose that the inhibition could be the result of the OdhI FHA domain binding to OdhA. O'Hare et al. (2008) showed that a *M. tuberculosis* GarA mutant with no phosphopeptide binding property in which the crucial FHA residue Ser95 is substituted by Ala failed to inhibit its target protein, KGD. This result clearly strengthens our assumption that the unmasked FHA domain in OdhI is required to promote binding to OdhA. However, the phosphorylation of OdhA remains to be established, as STPKs phosphorylation is a prerequisite for FHA recognition—even if preliminary experiments in *M. tuberculosis* suggest that the recombinant OdhA homolog expressed in *E. coli* (unlikely to be phosphorylated) is inhibited by GarA (O'Hare et al., 2008). Nevertheless, if OdhA phosphorylation is confirmed, this mechanism of regulation would lead to a double control on the OdhA enzyme activity by STPKs. In other words, phosphorylation of the OdhA enzyme would lead to its inhibition via binding with the unphosphorylated OdhI isoform, and phosphorylation of OdhI would release that inhibition on OdhA (Figure 7). Finally, an extensive analysis of OdhA/KGD phosphorylation by different STPKs would be of great interest to decipher the cross-talk networks used by the bacterium to adapt its response to external stimuli corresponding to environmental changes on the same metabolic pathway.

Our study unambiguously determined Thr15 as the unique phosphorylation site when OdhI is phosphorylated by *Cg*PknA or *Cg*PknB, and this was further confirmed by mass spectrometry and NMR analyses. It was previously reported that *Cg*PknG phosphorylates OdhI on Thr14 (Niebisch et al., 2006; Schultz et al., 2007). This strongly confirms that phosphorylation is site specific and dependent on the kinase, as already observed with the *M. tuberculosis* homolog GarA. In fact, similar observations have been reported for GarA, for which Thr22 was identified following treatment with PknB (which corresponds to Thr15 in OdhI, while Thr21 was the site identified following treatment with PknG (which corresponds to Thr14 in OdhI; Figure 1). It is noteworthy that multiple phosphorylation sites have been described in eukaryotic phosphopeptide-binding FHA domains (Byeon et al., 2005; Lee et al., 2008). For instance, double phosphorylation of the Rad53-SCD1 peptide increases affinity to the Dun1-FHA domain by more than two orders of magnitude, compared with a single phosphorylation. However, in that case, multiple phosphorylation events occurred simultaneously in Rad53-SCD1, whereas phosphorylation by either PknA/B or PknG on GarA was mutually exclusive (O'Hare et al., 2008).

In *M. tuberculosis* it has been shown that phosphorylation on both sites leads to the loss of the inhibition and binding properties (O'Hare et al., 2008). Sequences of the loop responsible for the phosphopeptide recognition are strictly identical between GarA and OdhI (Figure S2). Moreover, the N-terminal sequences are strictly conserved between OdhI and GarA around the pThr (position −4 to +6), corresponding to a larger motif than the usual

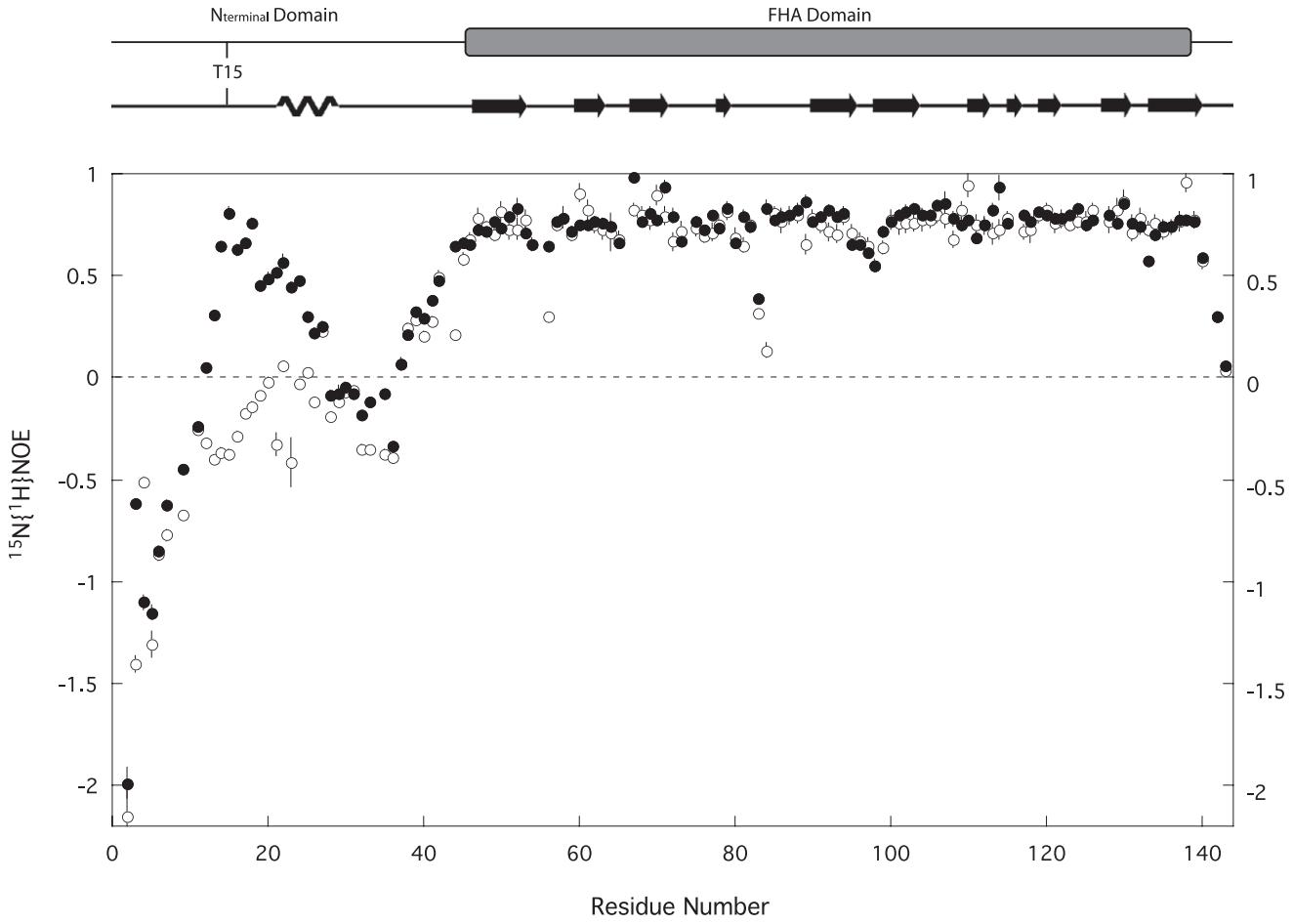

Figure 6. OdhI Isoforms Intrinsic Dynamics

$^{15}N\{^{1}H\}$ NOEs measured at 20°C for OdhI (open circles) and pOdhI (filled circles) as a function of the protein sequence. Protein domain delimitation and secondary element assignment for the phosphorylated form of OdhI are represented on the top.

residues described as essential for FHA binding (Durocher et al., 2000). This indicates that the structural rearrangement observed on pOdhI after phosphorylation by *Cg*PknA/B on Thr15 should be similar to the ones expected after phosphorylation on the adjacent Thr14 position while phosphorylated with *Cg*PknG, and this in order to abolish the inhibition on OdhA. In fact, the structure of pOdhI revealed that flexibility exists within the N-terminal domain between residues Arg19 to Glu38 (Figure 6). As a consequence, phosphorylation at position Thr14 could lead to a similar molecular switch. A model of pOdhI phosphorylated at position Thr14 reveals that the contact between the FHA binding site and the phosphorylated N-terminal would be possible with minor rearrangements of the phosphopeptide binding loops. With phosphorylation at position Thr14 instead of Thr15, the side chain of residue pThr +3 would be a valine (Val17) instead of a phenylalanine (Phe18), making all the hydrophobic interactions observed around this position practical. It is noteworthy that FHA domains are grouped into discrete classes primarily on the basis of pThr +3 specificity (Yaffe and Smerdon, 2004). Similarly, a substitution at position pThr +2 from valine (Val17) to serine (Ser16), and at position pThr +1 from serine (Ser16) to threonine (Thr15), should be compatible with the binding, as the interaction between this phosphopeptide segment and the FHA binding region involves mainly backbone atoms. At position pThr +1, the threonine (Thr14) would be substituted by a glutamic acid (Glu13), but this substitution should not generate any effect as the side chain is fully exposed to the solvent and does not interact with the binding region. From our model, the Glu13 Cβ and Cγ methylene groups make hydrophobic contacts with Val85 side chain; therefore, substituting Glu13 at position –2 with a valine residue (Val12) might increase the binding.

Despite our efforts, we never obtained an NMR sample of the pOdhI protein phosphorylated at position Thr14 by *Cg*PknG. This is probably due to the high instability of *Cg*PknG and the fact that this protein needs to be phosphorylated by *Cg*PknA/B to be activated. The ability of the OdhI/GarA protein to be a common substrate of two different kinases able to phosphorylate at two adjacent positions, and thus resulting in a similar major structural modification with the loss of inhibition properties, is remarkable considering the high specificity of the FHA domain phosphopeptide binding site (Durocher et al., 2000; Yaffe and Smerdon, 2004).

Control of enzyme activity by phosphorylation has been reported recently in actinomycetes (Bhatt et al., 2007), but to our knowledge, the OdhA regulation by OdhI is the first reported

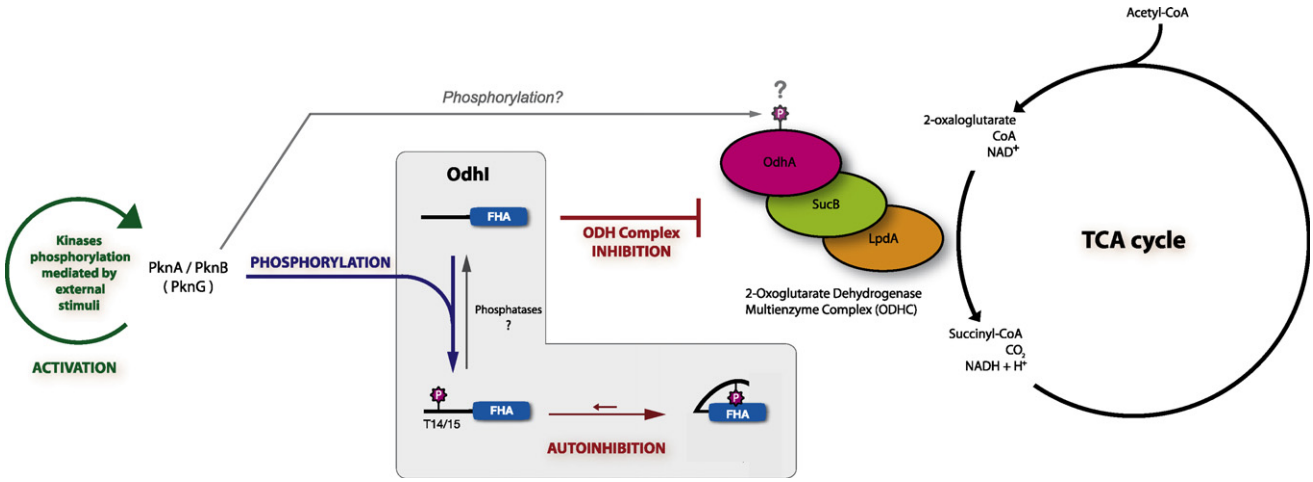

Figure 7. Proposed Regulatory Role of the Different Isoforms of OdhI as a Molecular Switch in Regulation of the Krebs (TCA) Cycle

The OdhI protein is a Krebs cycle key regulator in *C. glutamicum*. The unphosphorylated form of OdhI inhibits the fourth step of the cycle, and the phosphorylated form is inactive. Experimental evidence from NMR analysis unraveled a major conformational change between the two isoforms, leading to the binding of the phosphorylated N-terminal part of the protein to its own FHA domain, consequently inhibiting it, thus corresponding to an autoinhibition mechanism.

case of a bacterial enzyme controlled by phosphorylation via a second partner. In *M. tuberculosis*, for instance, there is an increasing number of processes found to be controlled by phosphorylation. Phosphorylation of the inhibitory protein (i.e., OdhI) and its target protein (i.e., OdhA) by a different set of kinases would allow bacteria to diversify and combine responses to diverse external stimuli received by different STPKs. One can also imagine that inhibitory protein (i.e., OdhI) could also recognize and therefore regulate additional targets. With a relatively restricted number of STPKs, the use of regulators like the OdhI/GarA protein, common to multiple pathways, could represent a way for the bacteria to extend its STPK regulation pathways.

Overall, our study describes for the first time a FHA domain phosphorylation-dependent regulation that leads to a functional alteration, and consequently to the inactivation, of its inhibitory properties. The FHA domain is a structural domain widespread in proteins involved in major eukaryotic cell processes. Moreover, phosphorylation of OdhI occurs in a complete disordered domain and leads to the complete loss of its properties, which is similar to eukaryotic proteins, as inhibition often involves phosphorylation of an unfolded part of the protein. This original autoinhibitory mechanism via a competitive intramolecular binding could be compared with the one observed for the eukaryotic SH2 domain protein (Kuriyan and Cowburn, 1997). Our findings may therefore not be restricted to the exclusive prokaryotic FHA domain proteins, but may represent a more general mechanism of post-translational regulation. The unexpected role of OdhI/GarA as a general molecular switch also emphasizes the fact that FHA domains should not be considered as solely protein-protein interaction domains but also as important activation/inhibition modules participating in prokaryotic and eukaryotic signaling.

EXPERIMENTAL PROCEDURES

Expression and Purifications of the OdhI Protein

A 50 ml falcon tube containing 20 ml of L-broth (1% w/v tryptone, 0.5% w/v NaCl, 0.5% w/v yeast extract) supplemented with 100 μg/ml of ampicillin was inoculated with a single transformed bacterial colony of *Escherichia coli* BL21(DE3)Star, harboring a variant of His-tag fusion vector pET-15b, which was modified to contain the *odhI* gene from *Corynebacterium glutamicum* and a tobacco etch virus (TEV) protease site to replace the thrombin site coding sequence (named pET-15b-Tev). This culture was grown in an orbital incubator set at 37°C and 220 rpm overnight. From this culture, the 20 ml was used to inoculate a 2-liter flask containing 750 ml of L-broth supplemented as before with ampicillin. The culture was grown in an orbital incubator set at 37°C and 220 rpm, until the A_{600} of the culture reached 0.6, and then IPTG was added at a final concentration of 0.2 mM to induce the expression of OdhI. Growth of the cultures was continued for a further 3 hr at a lower temperature of 30°C, after which the cells were harvested by centrifugation (using a Beckman Coulter Avanti J-20 XP centrifuge equipped with a 10 500 rotor and set at 7°C and 8000 rpm). The cell pellet arising from the 750 ml of culture was resuspended, on ice, in 30 ml of buffer A (50 mM Tris-HCl [pH 8.5], 150 mM NaCl) and 50 μl of 10 mg/ml lysozyme was added to aid in digestion of the cells. Cell pellets were stored at −80°C until required.

Cells were then lysed by sonication (2 s bursts for 5 min, at 60% amplitude, with a large parallel probe; Vibra Cell™ 72405 (Bioblock Scientific, Illkirch, France), after which cell debris and insoluble materials were removed by centrifugation (using a Beckman Coulter Avanti J-20 XP centrifuge equipped with a 25 50 rotor, set at 18,000 rpm, at 7°C). The supernatant arising from this step was filtered through a 0.22 μm PVDF filter (Millipore) and then loaded through a AKTA basic system into a Hitrap™ 1 ml IMAC HP column (Amersham Biosciences) equilibrated in buffer A and 4% of buffer B (50 ml of buffer A supplemented with 500 mM of imidazole). Ni^{2+}-agarose affinity chromatography was then carried out at room temperature to purify the His-tagged recombinant protein. The column was washed with successive applications of buffer A and 4% of buffer B (~30 ml in total) to remove all the impurities and then buffer B was increased over 20 ml to 100%, which was collected in fractions of 0.5 ml. Fractions containing the OdhI protein were identified by SDS-PAGE, then pooled and concentrated, using a 5 K cutoff concentrator, to a final volume of 5 ml (using a Sigma Laborzentrifugen 3K15 bioblock scientific centrifuge set at 7°C, 4000 g). The concentrated protein was applied to a Hiprep™ 26/10 (Amersham Biosciences) desalting column equilibrated in buffer A, to remove the imidazole, to increase protein stability. The first two 5 ml fractions eluted corresponded to the protein and so were pooled (total volume 10 ml) and placed in a labeled 15 ml falcon tube. The solution was treated for 2 hr at room temperature with TEV protease (~1 OD of TEV for 100 OD of protein) to digest and thereby remove the N-terminal His-tag from the protein.

Finally, the 10 ml of protein was concentrated (as before) to a final volume of 2 ml and applied to a Superdex 75 26/60 (Amersham Biosciences) size exclusion column, equilibrated in buffer 20 mM Na phosphate (pH 6.2), 150 mM NaCl. This led to the removal of any remaining impurities and the tag. Again,

fractions containing the OdhI protein were identified by SDS-PAGE, then pooled and stored at −20°C until required.

This protocol was carried out for all nonlabeled constructs of OdhI and ^{15}N-labeled OdhI constructs except the cultures, which were grown in a minimum media containing $^{15}NH_4Cl$ and ^{13}C6 glucose as the sole nitrogen and carbon sources.

Expression and Purification of *Cg*PknA and *Cg*PknB

E. coli BL21(DE3)Star cells were transformed with the pGEX4T-3 vector derivatives expressing the *Cg*PknA and *Cg*PknB core domain proteins (Fiuza et al., 2008). Recombinant *E. coli* strains harboring the pGEX4T-3 derivatives were used to inoculate 200 ml of LB medium supplemented with ampicillin and incubated at 37°C with shaking until A600 reached 0.5. Isopropyl 1-thio-β-D-galactopyranoside was then added at a final concentration of 0.5 mM, and growth was continued for an additional 3 hr period at 30°C. The cells were harvested by centrifugation at 6000 g for 10 min, washed in 10 ml of buffer A (50 mM Tris-HCl [pH 7.5], 150 mM NaCl, 10% glycerol, 1 mM EDTA, 1 mM aprotinin), and centrifuged again under the same conditions. The cell pellet was resuspended in buffer A containing DNase I and RNase A at a final concentration of 5 g/ml each, 10 M leupeptin, and 6 M pepstatin.

Cells were disrupted in a French pressure cell at 16,000 lb/in^2 (psi). The resulting suspension was centrifuged at 4 C for 30 min at 30,000 g. The supernatant was incubated for 5 hr with glutathione Sepharose 4B matrix (Pharmacia Biotech), suitable for purification of GST fusion proteins. The protein-resin complex was packed into a column for washing and elution. The column was washed with 50 ml of PBS. Protein elution was carried out with buffer B (50 mM Tris-HCl [pH 8.0], 5 mM MgCl2, 1 mM DTT) containing 15 mM glutathione. Eluted fractions were analyzed by SDS-PAGE. After dialysis against buffer C (40 mM Tris-HCl [pH 7.9], 200 mM NaCl, 0.2 mM DTT, 0.2 mM EDTA, 10% glycerol), pure fractions were pooled. All proteins were purified under the same conditions, and their identity was checked by mass spectrometry (MALDI-TOF).

Phosphorylation of OdhI by *Cg*PknA and *Cg*PknB

In vitro phosphorylation of each recombinant OdhI sample (5 mg) was carried out overnight at 37°C in a reaction mixture containing buffer 25 mM Tris-HCl (pH 7.0), 1 mM dithiothreitol, 5 mM MgCl2, 1 mM EDTA, and 5 mM ATP and 1 mg of kinases (*Cg*PknA and *Cg*PknB). The sample was then concentrated and applied to a Superdex 75 10/30 (Amersham Biosciences) size exclusion column, equilibrated in buffer 20 mM Na phosphate (pH 6.2), 150 mM NaCl. Fractions containing the OdhI protein were identified by SDS-PAGE, then pooled and stored and concentrated to a concentration of approximately 500 μM for NMR experiments.

Mass Spectrometry Analysis

Purified OdhI was subjected to in vitro phosphorylation as described. Subsequent mass spectrometry analyses were performed as previously described (Fiuza et al., 2008).

Solution Structure of OdhI and pThr15-OdhI

All NMR experiments were carried out at 14.1 Tesla on a Bruker Avance 600 spectrometer equipped with 5 mm *z*-gradient ^{1}H-^{13}C-^{15}N triple-resonance cryoprobe. ^{1}H, ^{13}C, and ^{15}N resonances were assigned using standard triple-resonance 3D experiments (Sattler et al., 1999) recorded at 20°C on 0.3 mM ^{15}N- or ^{15}N,^{13}C-labeled OdhI protein samples dissolved in 20 mM sodium phosphate (pH 6.2), 150 mM NaCl with 5% D_2O for the lock. ^{1}H chemical shifts were directly referenced to the methyl resonance of DSS, whereas ^{13}C and ^{15}N chemical shifts were referenced indirectly to the absolute frequency ratios ^{15}N/^{1}H = 0.101329118 and ^{13}C/^{1}H = 0.251449530. All NMR spectra were processed with GIFA software (Pons et al., 1996). NOE peaks identified on 3D [^{1}H,^{15}N] and [^{1}H,^{13}C] 3D NOESY-HSQC were assigned through automated NMR structure calculations with CYANA 2.1 (Guntert, 2004).

Pulse sequences similar to those described (Kay et al., 1992; Peng and Wagner, 1992a, 1992b) were used to record heteronuclear ^{15}N{^{1}H}NOE experiments. The two experiments with and without proton saturation were acquired in an interleaved manner, FID by FID. Proton saturation was achieved by application of high-power 120° pulse spaced at 20 ms intervals for 3 s prior to the first pulse on ^{15}N. A relaxation delay equal to 6 s between each scan was used to obtain a complete relaxation of water magnetization and to reduce effects arising from amide proton exchange.

Backbone ϕ and ψ torsion angle constraints were obtained from a database search procedure on the basis of backbone (^{15}N, HN, $^{13}C'$, $^{13}C^{\alpha}$, H^{α}, $^{13}C^{\beta}$) chemical shifts using the program TALOS (Cornilescu et al., 1999). Hydrogen bond restraints were derived using standard criteria on the basis of the amide ^{1}H / ^{2}H exchange experiments and NOE data. When identified, the hydrogen bond was enforced using the following restraints: ranges of 1.8–2.3 Å for *d*(N-H,O), and 2.7–3.3 Å for *d*(N,O). The final list of restraints (from which values redundant with the covalent geometry has been eliminated) consisted of 290 intraresidues, 445 sequential, 63 medium-range ($1 < i\text{-}j \leq 4$), and 225 long-range upper-bound distance restraints, 156 backbone dihedral angle restraints (ϕ and φ), and 60 hydrogen bond restraints. The phosphothreonine parameters were incorporated according the phosphorylated amino acid library from Craft and Legge (2005). The 30 best structures (based on the final target penalty function values) were minimized with CNS 1.2 according the RECOORD procedure (Nederveen et al., 2005) and analyzed with PROCHECK (Laskowski et al., 1993). The rms deviations were calculated with MOLMOL (Koradi et al., 1996). Structural statistics are given as Supplemental Data (Table 1).

Table 1. NMR and Refinement Statistics for OdhI Protein Structures

	OdhI	pOdhI
NMR distance and dihedral constraints		
Distance constraints		
Total NOE	976	997
Intraresidue	269	279
Interresidue		
Sequential (|i − j| = 1)	431	428
Medium-range (|i − j| < 4)	76	59
Long range (|i − j| > 5)	200	231
Intermolecular		
Hydrogen bonds	60	60
Total dihedral angle restraints		
φ	55	106
ψ	55	106
Structure statistics		
Violations (mean and SD)		
Max. dihedral angle violation (°)	3.33 ± 1.11	4.04 ± 1.05
Max. distance constraint violation (Å)	0.16 ± 0.04	0.16 ± 0.04
Deviations from idealized geometry		
Bond lengths (Å)	0.012 ± 0.001	0.011 ± 0.001
Bond angles (°)	1.220 ± 0.031	1.199 ± 0.028
Impropers (°)	1.647 ± 0.101	1.572 ± 0.098
Ramachandran plot (%)		
Most favored region	80.7	87.3
Additionally allowed region	17.2	11.8
Generously allowed region	1.6	0.5
Disallowed region	0.5	0.4
Average pairwise rmsd[a] (Å)		
Backbone atoms	1.09 ± 0.23	0.74 ± 0.13
Heavy atoms	1.92 ± 0.24	1.45 ± 0.16

[a] Pairwise rmsd was calculated among 30 refined structures for residues 48–71, 90–102, and 119–138.

ACCESSION NUMBERS

Structure coordinates for OdhI and pOdhI have been deposited in the Protein Data Bank (www.rcsb.org/pdb/) with entry codes 2kb4 and 2kb3. Chemical shifts have been deposited in the BioMagResBank under accession numbers BMRB-16039 and BMRB-16038.

SUPPLEMENTAL DATA

Supplemental Data include three figures and can be found with this article online at http://www.cell.com/structure/supplemental/S0969-2126-(09)00094-X.

ACKNOWLEDGMENTS

NMR experiments were recorded and analyzed using the facilities of the Structural Biology platform RIO (Centre de Biochimie Structurale, Montpellier, France). We thank Gilles Labesse and the Atelier de Bio and Chimie Informatique Structurale team (http://abcis.cbs.cnrs.fr) for their helpful discussions, and Andrea Lee for her kind corrections. The authors also thank M. Becchi, I. Zanella-Cléon, and A. Cornut (Institut de Biologie et Chimie des Proteines, Lyon, France) for their excellent expertise and technical assistance in mass spectrometry analysis. This work was supported by the Agence National de la Recherche (Grant JC07_203251 to M.C.-G. and ANR-06-MIME-027-01 to V.M.).

Received: November 21, 2008
Revised: February 4, 2009
Accepted: February 7, 2009
Published: April 14, 2009

REFERENCES

Alderwick, L.J., Radmacher, E., Seidel, M., Gande, R., Hitchen, P.G., Morris, H.R., Dell, A., Sahm, H., Eggeling, L., and Besra, G.S. (2005). Deletion of Cg-emb in corynebacterianeae leads to a novel truncated cell wall arabinogalactan, whereas inactivation of Cg-ubiA results in an arabinan-deficient mutant with a cell wall galactan core. J. Biol. Chem. *280*, 32362–32371.

Bhatt, A., Molle, V., Besra, G.S., Jacobs, W.R., Jr., and Kremer, L. (2007). The mycobacterium tuberculosis FAS-II condensing enzymes: their role in mycolic acid biosynthesis, acid-fastness, pathogenesis and in future drug development. Mol. Microbiol. *64*, 1442–1454.

Bott, M. (2007). Offering surprises: TCA cycle regulation in Corynebacterium glutamicum. Trends Microbiol. *15*, 417–425.

Byeon, I.J., Li, H., Song, H., Gronenborn, A.M., and Tsai, M.D. (2005). Sequential phosphorylation and multisite interactions characterize specific target recognition by the FHA domain of Ki67. Nat. Struct. Mol. Biol. *12*, 987–993.

Cornilescu, G., Delaglio, F., and Bax, A. (1999). Protein backbone angle restraints from searching a database for chemical shift and sequence homology. J. Biomol. NMR *13*, 289–302.

Craft, J.W., Jr., and Legge, G.B. (2005). An AMBER/DYANA/MOLMOL phosphorylated amino acid library set and incorporation into NMR structure calculations. J. Biomol. NMR *33*, 15–24.

Cozzone, A.J. (1998). Regulation of acetate metabolism by protein phosphorylation in enteric bacteria. Annu. Rev. Microbiol. *52*, 127–164.

Durocher, D., and Jackson, S.P. (2002). The FHA domain. FEBS Lett. *513*, 58–66.

Durocher, D., Taylor, I.A., Sarbassova, D., Haire, L.F., Westcott, S.L., Jackson, S.P., Smerdon, S.J., and Yaffe, M.B. (2000). The molecular basis of FHA domain: phosphopeptide binding specificity and implications for phospho-dependent signaling mechanisms. Mol. Cell *6*, 1169–1182.

England, P., Wehenkel, A., Martins, S., Hoos, S., Andre-Leroux, G., Villarino, A., and Alzari, P.M. (2009). The FHA-containing protein GarA acts as a phosphorylation-dependent molecular switch in mycobacterial signaling. FEBS Lett. *583*, 301–307.

Fiuza, M., Canova, M.J., Zanella-Cleon, I., Becchi, M., Cozzone, A.J., Mateos, L.M., Kremer, L., Gil, J.A., and Molle, V. (2008). From the characterization of the four serine/threonine protein kinases (PknA/B/G/L) of corynebacterium glutamicum toward the role of PknA and PknB in cell division. J. Biol. Chem. *283*, 18099–18112.

Guntert, P. (2004). Automated NMR structure calculation with CYANA. Methods Mol. Biol. *278*, 353–378.

Huen, M.S., Grant, R., Manke, I., Minn, K., Yu, X., Yaffe, M.B., and Chen, J. (2007). RNF8 transduces the DNA-damage signal via histone ubiquitylation and checkpoint protein assembly. Cell *131*, 901–914.

Kalinowski, J., Bathe, B., Bartels, D., Bischoff, N., Bott, M., Burkovski, A., Dusch, N., Eggeling, L., Eikmanns, B.J., Gaigalat, L., et al. (2003). The complete Corynebacterium glutamicum ATCC 13032 genome sequence and its impact on the production of L-aspartate-derived amino acids and vitamins. J. Biotechnol. *104*, 5–25.

Kay, L.E., Nicholson, L.K., Delaglio, F., Bax, A., and Torchia, D.A. (1992). Pulse sequences for removal of the effects of cross correlation between dipolar and chemical-shift anisotropy relaxation mechanisms on the measurement of heteronuclear T1 and T2 values in proteins. J. Magn. Reson. *97*, 359–375.

Kimura, E. (2003). Metabolic engineering of glutamate production. Adv. Biochem. Eng. Biotechnol. *79*, 37–57.

Koradi, R., Billeter, M., and Wuthrich, K. (1996). MOLMOL: a program for display and analysis of macromolecular structures. J. Mol. Graph. *14*, 51–55, 29–32.

Kuriyan, J., and Cowburn, D. (1997). Modular peptide recognition domains in eukaryotic signaling. Annu. Rev. Biophys. Biomol. Struct. *26*, 259–288.

Laskowski, R.A., Moss, D.S., and Thornton, J.M. (1993). Main-chain bond lengths and bond angles in protein structures. J. Mol. Biol. *231*, 1049–1067.

Lee, H., Yuan, C., Hammet, A., Mahajan, A., Chen, E.S., Wu, M.R., Su, M.I., Heierhorst, J., and Tsai, M.D. (2008). Diphosphothreonine-specific interaction between an SQ/TQ cluster and an FHA domain in the Rad53-Dun1 kinase cascade. Mol. Cell *30*, 767–778.

Li, H., Byeon, I.J., Ju, Y., and Tsai, M.D. (2004). Structure of human Ki67 FHA domain and its binding to a phosphoprotein fragment from hNIFK reveal unique recognition sites and new views to the structural basis of FHA domain functions. J. Mol. Biol. *335*, 371–381.

Li, J., Williams, B.L., Haire, L.F., Goldberg, M., Wilker, E., Durocher, D., Yaffe, M.B., Jackson, S.P., and Smerdon, S.J. (2002). Structural and functional versatility of the FHA domain in DNA-damage signaling by the tumor suppressor kinase Chk2. Mol. Cell *9*, 1045–1054.

Nederveen, A.J., Doreleijers, J.F., Vranken, W., Miller, Z., Spronk, C.A., Nabuurs, S.B., Guntert, P., Livny, M., Markley, J.L., Nilges, M., et al. (2005). RECOORD: a recalculated coordinate database of 500+ proteins from the PDB using restraints from the BioMagResBank. Proteins *59*, 662–672.

Niebisch, A., Kabus, A., Schultz, C., Weil, B., and Bott, M. (2006). Corynebacterial protein kinase G controls 2-oxoglutarate dehydrogenase activity via the phosphorylation status of the OdhI protein. J. Biol. Chem. *281*, 12300–12307.

O'Hare, H.M., Duran, R., Cervenansky, C., Bellinzoni, M., Wehenkel, A.M., Pritsch, O., Obal, G., Baumgartner, J., Vialaret, J., Johnsson, K., et al. (2008). Regulation of glutamate metabolism by protein kinases in mycobacteria. Mol. Microbiol. *98*, 308–332.

Peng, J.W., and Wagner, G. (1992a). Mapping of the spectral densities of N-H bond motions in eglin c using heteronuclear relaxation experiments. Biochemistry *31*, 8571–8586.

Peng, J.W., and Wagner, G. (1992b). Mapping of the spectral density functions using heteronuclear NMR relaxation experiments. J. Magn. Reson. *98*, 308–332.

Pons, J.L., Malliavin, T.E., and Delsuc, M.A. (1996). Gifa V 4: a complete package for NMR data set processing. J. Biomol. NMR *8*, 445–452.

Sattler, M., Schleucher, J., and Griesinger, C. (1999). Heteronuclear multidimensional NMR experiments for the structure determination of proteins in solution employing pulsed field gradients. Prog. Nucl. Magn. Reson. Spectrosc. *34*, 93–158.

Schultz, C., Niebisch, A., Gebel, L., and Bott, M. (2007). Glutamate production by Corynebacterium glutamicum: dependence on the oxoglutarate

 ©2009 Elsevier Ltd All rights reserved

dehydrogenase inhibitor protein OdhI and protein kinase PknG. Appl. Microbiol. Biotechnol. *76*, 691–700.

Villarino, A., Duran, R., Wehenkel, A., Fernandez, P., England, P., Brodin, P., Cole, S.T., Zimny-Arndt, U., Jungblut, P.R., Cervenansky, C., et al. (2005). Proteomic identification of M. tuberculosis protein kinase substrates: PknB recruits GarA, a FHA domain-containing protein, through activation loop-mediated interactions. J. Mol. Biol. *350*, 953–963.

Yaffe, M.B., and Smerdon, S.J. (2004). The use of in vitro peptide-library screens in the analysis of phosphoserine/threonine-binding domain structure and function. Annu. Rev. Biophys. Biomol. Struct. *33*, 225–244.

 ©2009 Elsevier Ltd All rights reserved